Realization of Expeditious Layer-by-Layer Siloxane-Based Self-assembly as an Efficient Route to Structurally Regular Acentric Superlattices with Large Electro-optic Responses

Peiwang Zhu,[†] Milko E. van der Boom,[†,§] Hu Kang,[†] Guennadi Evmenenko,[‡] Pulak Dutta,[‡] and Tobin J. Marks*[,†]

Department of Chemistry and the Materials Research Center, and Department of Physics and Astronomy and the Materials Research Center, Northwestern University, Evanston, Illinois 60208-3113

Received May 7, 2002. Revised Manuscript Received August 29, 2002

A new, expeditious siloxane-based layer-by-layer assembly process for the formation of intrinsically polar organic electro-optic thin films is described using highly reactive $-SiCl_2I$-functionalized, silyl-protected donor−acceptor azo-benzene chromophore derivatives and octachlorotrisiloxane as a deprotecting reagent/interlayer precursor. This all-"wet-chemical" two-step process can be efficiently implemented in a vertical dipping procedure to yield polar films consisting of 40 alternating chromophore and capping layers. Each nanoscale bilayer (chromophore + polysiloxane layer ≈ 3.26-nm thick) can be grown in ≈40 min—at least 1 order of magnitude more rapidly than previous siloxane-based solution deposition methodologies. Chromophore monolayer deposition from solution reaches completion in ≈15 min at 55 °C. The adherent, structurally regular assemblies exhibit appreciable electro-optic responses ($\chi^{(2)} \sim 180$ pm/V and $r_{33} \sim 65$ pm/V determined by SHG measurements at 1064 nm) and high chromophore surface densities (≈40 Å^2/chromophore) and have been characterized by a full complement of physicochemical techniques: optical spectroscopy, aqueous contact-angle measurements, specular X-ray reflectivity, atomic force microscopy, and angle-dependent polarized second-harmonic generation.

Introduction

The formation of functional nanoscale multimolecular organizates (e.g., thin films, molecular wires, molecular dots, etc.)[1,2] and the efficient translation of molecular properties/functions into macroscopic observables/responses by developing new growth and self-assembly techniques are topics of great current interest.[1−5] Furthermore, a high level of structural control at nanoscale dimensions is a necessary requirement to exert full control over numerous materials properties (e.g., optoelectronic, charge transport, and magnetic). Many factors at the molecular level (e.g., molecular architecture and electronic structure, reactivity, electrostatics, hydrogen bonding, and van der Waals interactions) play an essential role in the design and buildup of structures with elaborate architectural complexity. Crystal engineering,[1,3] Langmuir−Blodgett (LB) deposition,[4] and self-assembly (SA) and self-organization[1,5] are only a few contemporary examples of the many rational approaches to amplifying molecular properties and inducing order and intermolecular communication in condensed molecular matter. In this regard, the formation of device-quality photonic molecular materials represents one promising direction in the scientific quest to

* To whom correspondence should be addressed. E-mail: tjmarks@casbah.acns.nwu.edu.

[†] Department of Chemistry and the Materials Research Center.

[‡] Department of Physics and Astronomy and the Materials Research Center.

[§] Present address: Department of Organic Chemistry, The Weizmann Institute of Science, Rehovot, 76100, Israel.

(1) For recent reviews, see: (a) Lehn, J. M. *Science* **2002**, *295*, 2400−2403. (b) Reinhoudt, D. N.; Crego-Calama, M. *Science* **2002**, *295*, 2403−2407. (c) Ikkala, O.; ten Brinke, G. *Science* **2002**, *295*, 2407−2409. (d) Hollingsworth, M. D. *Science* **2002**, *295*, 2410−2413. (e) Kato, T. *Science* **2002**, *295*, 2414−2418. (f) Whitesides, G. M.; Grzybowski, B. *Science* **2002**, *295*, 2418−2421.

(2) For recent reviews, see: (a) Stoddart, J. F. *Acc. Chem. Res.* **2001**, *34*, 410−522 (special issue on molecular machines). (b) Kuzmenko, I.; Rapaport, H.; Kjaer, K.; Als-Nielsen, J.; Weissbuch, I.; Lahav, M.; Leiserowitz, L. *Chem. Rev.* **2001**, *101*, 1659−1696. (c) Swager, T. M. *Acc. Chem. Res.* **1998**, *31*, 201−207. (d) Atwood, J. L., Davies, J. E. D., Macnicol, D. D., Vogtle, F., Eds.; *Comprehensive Supramolecular Chemistry*; Pergamon Press: New York, 1996. (e) Lehn, J.-M. *Supramolecular Chemistry*: *Concepts and Perspectives*; VCH: New York, 1995.

(3) (a) Evans, O. R.; Lin, W. *Acc. Chem. Res.* **2002**, *35*, 511−522. (b) Dotan, N.; Arad, D.; Frolow, F.; Freeman, A. *Angew. Chem., Int. Ed.* **1999**, *38*, 2363−2366. (c) Moulton, B.; Zaworotko, M. J. *Chem. Rev.* **2001**, 1629−1658. (d) Desiraju, G. R. *Crystal Engineering: the Design of Organic Solids*: Elsevier: New York, 1989.

(4) (a) Schwartz, H.; Mazor, R.; Khodorkovsky, V.; Shapiro, L.; Klug, J. T.; Kovalev, E.; Meshulam, G.; Berkovic, G.; Kotler, Z.; Efrima, S. *J. Phys. Chem. B* **2001**, *105*, 5914−5921. (b) Ricceri, R.; Neto, C.; Abbotto, A.; Facchetti, A.; Pagani, G. A. *Langmuir* **1999**, *15*, 2149−2151. (c) Roberts, M. J.; Lindsay, G. A.; Herman, W. N.; Wynne, K. J. *J. Am. Chem. Soc.* **1998**, *120*, 11202−11203. (d) Wijekoon, W. M. K. P.; Wijayu, S. K.; Bhawalkar, J. D.; Prasad, P. N.; Penner, T. L.; Armstrong, N. J.; Ezenyilimba, M. C.; Williams, D. J. *J. Am. Chem. Soc.* **1996**, *118*, 4480−4483. (e) Ashwell, G. J.; Jackson, P. D.; Crossland, W. A. *Nature* **1994**, *368*, 438−440.

(5) Weissbuch, I.; Baxter, P. N. W.; Cohen, S.; Cohen, H.; Kjaer, K.; Howes, P. B.; Als-Nielsen, J.; Hanan, G. S.; Schubert, U. S.; Lehn, J.-M.; Leiserowitz, L.; Lahav, M. *J. Am. Chem. Soc.* **1998**, *120*, 4850−4860.

10.1021/cm020438t CCC: $22.00
Published on Web 10/29/2002

gain greater temporal and spacial control over the propagation of light waves in the condensed state. Molecular electro-optic materials offer a particular synthetic challenge since organizing large hyperpolarizability (hence dipolar) building blocks into *acentric microstructures* doubtless incurs large thermodynamic challenges.[6,7] Nevertheless, substantial progress has been made using electric field processing of glassy polymers,[8] Langmuir−Blodgett film growth,[4] and the self-assembly of covalently interconnected superlattices.[9−12] In addition to fundamental scientific motivation, the successful formation of high-response molecular assemblies with acceptable robustness, transparency, and processing characteristics could lead to novel low switching voltage/large bandwidth electro-optic (EO) light modulators and related devices, promising greatly increased rates of information transmission by enhancing speed, capacity, and bandwidth for optical data networking and telecommunications.[6,9−12]

For the above reasons, development of efficient synthetic approaches to the growth and modification of structurally elaborate photonically/electronically functional superlattices with excellent optical, thermal, and chemical properties is of particular scientific interest and potential utility.[6−12] Among the aforementioned, layer-by-layer chemisorptive siloxane-based self-assembly approaches[13] are particularly attractive because of the following: (i) Self-assembled superlattices (SASs) offer far higher EO coefficients and lower dielectric constants than established inorganic materials (e.g., $LiNbO_3$).[14] (ii) The chromophores are covalently linked to the substrates, and the films are closely packed and robust. (iii) Molecular orientation is intrinsically acentric, and postdeposition processing steps such as poling are not necessary. (iv) Chromophore orientation is locked into place with strong covalent cross-links; hence, the microstructural orientation is very stable. (v) Precise control of film refractive index can be achieved at the subwavelength molecular level. (vi) Large area films can be easily prepared. (vii) Chromophore arrays can be fabricated on silicon or a variety of related substrates, allowing ready device integration and therefore significantly reduced device design complexity.[15,16] The present systems are regarded as "self-assembing"[17a] in that they most likely derive from noncovalently bound precursor assemblies[17b] and the ultimate topotactic structures that are locked into place by self-limiting chemisorption/cross-linking are enforced by noncovalent cation−anion and van der Waals forces.[17c]

Previous contributions[9−12] from this laboratory described a three-step procedure to fabricate robust, acentric multilayer superlattices composed of stilbazolium and related chromophores, exhibiting very large NLO/EO responses ($\chi^{(2)}$ = 150−200 pm/V). Recently, SAS-based ultrafast frequency-selective switching devices,[15a] traveling wave evanescent mode EO-phase modulators[15b−d] (Scheme 1), and frequency-doubling devices[15e] have been fabricated with these materials, stimulating our interest in elaborating and refining layer-by-layer deposition methodologies for EO film growth. Since the thickness required for optimum single-mode waveguiding EO film devices should be ≈0.5 μm or more, at least 150 SAS trilayers (450 growth

(6) (a) Würthner, F.; Wortmann, R.; Meerholz, K. *ChemPhysChem* **2002**, *3*, 17−31. (b) Lacroix, P. G. *Eur. J. Inorg. Chem.* **2001**, 339−348. (c) Samijn, C.; Verbiest, T.; Persoons, A. *Macromol. Rapid Commun.* **2000**, *21*, 1−15. (d) Dalton, L. R.; Steier, W. H.; Robinson, B. H.; Zhang, C.; Ren, A.; Garner, S.; Chen, A.; Londergan, T.; Irwin, L.; Carlson, B.; Fifield, L.; Phelan, G.; Kincaid, C.; Amend, J.; Jen, A. *J. Mater. Chem.* **1999**, *9*, 1905−1920. (e) Steier, W. H.; Chen, A.; Lee, S.-S.; Garner, S.; Zhang, H.; Chuyanov, V.; Dalton, L. R.; Wang, F.; Ren, A. S.; Zhang, C.; Tordorova, G.; Harper, A.; Fetterman, H. R.; Chen, D.; Udupa, A.; Bhattacharya, D.; Tsap, B. *Chem. Phys.* **1999**, *245*, 487−506. (f) Marder, S. R.; Kippelen, B.; Jen, A. K. Y.; Peyghambarian, N. *Nature* **1997**, *388*, 845−851. (g) Long, N. J. *Angew. Chem., Int. Ed. Engl.* **1995**, *34*, 21−38. (h) Marks, T. J.; Ratner, M. *Angew. Chem., Int. Ed. Engl.* **1995**, *34*, 155−173. (i) *Chem. Rev.* special issue on "Optical Nonlinearities in Chemistry" (Burland, D. M., Ed.) **1994**, *94*, 1−278. (j) *Molecular Nonlinear Optics−Materials, Physics and Devices*; Zyss, J., Ed.; Academic Press: San Diego, CA, 1994.

(7) Lehn, J.-M. *Angew. Chem., Int. Ed. Engl.* **1988**, *27*, 89−112.

(8) (a) Ma, H.; Chen, B.; Sassa, T.; Dalton, L. R.; Jen, A. K.-Y. *J. Am. Chem. Soc.* **2001**, *123*, 986−987. (b) Shi, Y.; Zhang, C.; Zhang, H.; Bechtel, J. H.; Dalton, L. R.; Robinson, B. H.; Steier, W. H. *Science* **2000**, *288*, 199−122. (c) Yitzchaik, S.; Di Bella, S.; Lundquist, P. M.; Wong, G. K.; Marks, T. J. *J. Am. Chem. Soc.* **1997**, *119*, 2995−3002. (d) Ye, C.; Minami, N.; Marks, T. J.; Yang, J.; Wong, G. K. *Macromolecules* **1988**, *21*, 2899−2901. (e) Ye, C.; Marks, T. J.; Yang, J.; Wong, G. K. *Macromolecules* **1987**, *20*, 2322−2324. (f) van der Boom, M. E. *Angew. Chem. Int. Ed. Engl.* **2002**, *41*, 3363−3366.

(9) (a) van der Boom, M. E.; Zhu, P.; Evmenenko, G.; Malinsky, J. E.; Lin, W.; Dutta, P.; Marks, T. J. *Langmuir* **2002**, *18*, 3704−3707. (b) van der Boom, M. E.; Richter, A. G.; Malinsky, J. E.; Lee, P. A.; Armstrong, N. R.; Dutta, P.; Marks, T. J. *Chem. Mater.* **2001**, *13*, 15−17. (c) van der Boom, M. E.; Richter, A. G.; Malinsky, J. E.; Dutta, P.; Marks, T. J.; Lee, P. A.; Armstrong, N. R. *Polym. Mater. Sci. Eng.* **2000**, *83*, 160−161.

(10) van der Boom, M. E.; Evmenenko, G.; Dutta, P.; Marks, T. J. *Adv. Funct. Mater.* **2001**, *11*, 393−397.

(11) Evmenenko, G.; van der Boom, M. E.; Kmetko, J.; Dugan, S. W.; Marks, T. J.; Dutta, P. *J. Chem. Phys.* **2001**, *115*, 6722−6727.

(12) (a) Malik, A.; Lin, W.; Durbin, M. K.; Marks, T. J.; Dutta, P. *J. Chem. Phys.* **1997**, *107*, 645−651. (b) Lin, W.; Lee, T.-L.; Lyman, P. F.; Lee, J.; Bedzyk, M. J.; Marks, T. J. *J. Am. Chem. Soc.* **1997**, *119*, 2205−2211. (c) Lin, W.; Lin, W.; Wong, G. K.; Marks, T. J. *J. Am. Chem. Soc.* **1996**, *118*, 8034−8042. (d) Yitzchaik, S.; Marks, T. J. *Acc. Chem. Res.* **1996**, *29*, 197−202.

(13) For other examples of materials construction via layer-by-layer self-assembly see: (a) Doron-Mor, I.; Hatzor, A.; Vaskevich, A.; van der Boom-Moav, T.; Shanzer, A.; Rubinstein I.; Cohen, H. *Nature* **2000**, *406*, 382−385. (b) Neff, G. A.; Helfrich, M. R.; Clifton, M. C.; Page, C. J. *Chem. Mater.* **2000**, *12*, 2363−2371. (c) Frutos, A. G.; Brockman, J. M.; Corn, R. M. *Langmuir* **2000**, *16*, 2192−2197. (d) Flory, W. C.; Mehrens, S. M.; Blanchard, G. J. *J. Am. Chem. Soc.* **2000**, *122*, 7976−7985. (e) Hanken, D. G.; Naujok, R. R.; Gray, J. M.; Corn, R. M. *Anal. Chem.* **1997**, *69*, 240−248. (f) Fang, M.; Kaschak, D. M.; Sutorik, A. C.; Mallouk, T. E. *J. Am. Chem. Soc.* **1997**, *119*, 12184−12191. (g) Moaz, R.; Matlis, S.; DiMasi, E.; Ocko, B. M.; Sagiv, J. *Nature* **1996**, *384*, 150−153. (h) Collins, R. J.; Bae, I. T.; Scherson, D. A.; Sukenik, C. N. *Langmuir* **1996**, *12*, 5509−5111. (i) Katz, H. E.; Wilson, W. L.; Scheller, G. *J. Am. Chem. Soc.* **1994**, *116*, 6636−6640. (j) Katz, H. E.; Scheller, G.; Putvinski, T. M.; Schilling, M. L.; Wilson, W. L.; Chidsey, C. E. D. *Science* **1991**, *254*, 1485. (k) Li, D.-Q.; Ratner, M. A.; Marks, T. J.; Zhang, C.-H.; Yang, J.; Wong, G. K. *J. Am. Chem. Soc.* **1990**, *112*, 7389−7390. (l) Moaz, R.; Sagiv, J. *Langmuir* **1987**, *3*, 1034−1044. (m) Netzer, L.; Sagiv, J. *J. Am. Chem. Soc.* **1983**, *105*, 674−676.

(14) Woten, E. L.; Kissa, K. M.; Yi-Yan, A.; Murphy, E. J.; Lafaw, D. A.; Hallemeier, P. F.; Maack, D.; Attanasio, D. V.; Fritz, D. J.; McBrien, G. J.; Bossi, D. E. *IEEE, J. Sel. Topics Quantum Electron.* **2000**, *6*, 69−82, and references therein.

(15) (a) Wang, G.; Zhu, P.; Marks, T. J.; Ketterson, J. B. *Appl. Phys. Lett., Appl. Phys. Lett.*, **2002**, *81*, 2169−2171. (b) Zhao, Y.-G.; Chang, S.; Wu, A.; Lu, H.-L.; Ho, S.-T.; van der Boom, M. E.; Marks, T. J., *Opt. Eng. Lett.*, in press. (c) Zhao, Y.-G.; Wu, A.; Lu, H.-L.; Chang, S.; Lu, W.-K.; Ho, S.-T.; van der Boom, M. E.; Malinsky, J. E.; Marks, T. J. *Appl. Phys. Lett.* **2001**, *79*, 587−589. (d) van der Boom, M. E.; Malinsky, J. E.; Zhao, Y.-G.; Chang, S.; Lu, W. K.; Ho, S. T.; Marks, T. J. *Polym. Prepr.* (*Am. Chem. Soc., Div. Polym. Chem.*) **2001**, *42*, 550−551. (e) Lundquist, P. M.; Lin, W.; Zhou, H.; Hahn, D. N.; Yitzchaik, S.; Marks, T. J.; Wong, G. K. *Appl. Phys. Lett.* **1997**, *70*, 1941−1943.

(16) For poled polymer devices, see: (a) Zhang, H.; Oh, M.-C.; Szep, A.; Steier, W. H.; Zhang, C.; Dalton, L. R.; Erlig, H.; Chang, Y.; Chang, D. H.; Fetterman, *Appl. Phys. Lett.* **2001**, *78*, 3136−3138. (b) Shi, Y.; Zhang, C.; Zhang, H.; Bechtel, J. H.; Dalton, L. R.; Robinson, B. H.; Steier, W. H. *Science* **2000**, *288*, 199−122; (f) review: Dalton, L. R. *Opt. Eng.* **2000**, *39*, 589−595.

(17) (a) van der Veen, N. J.; Flink, S.; Deij, M. A.; Egberink, R. J. M.; van Veggel, F. C. J. M.; Reinhoudt, D. N. *J. Am. Chem. Soc.* **2000**, *122*, 6112−6113. (b) Richter, A. G.; Yu, C.-Y.; Datta, A.; Kmetko, J.; Dutta, R. *Phys. Rev. E* **2000**, *61*, 607−615. (c) For a review of such systems, see: Ulman, A. *Chem. Rev.* **1996**, *96*, 1533−1554.

Scheme 1. Schematic Cross Section of an SAS-Based Traveling Wave Electro-optic Phase Modulator (from Ref 15c)[a]

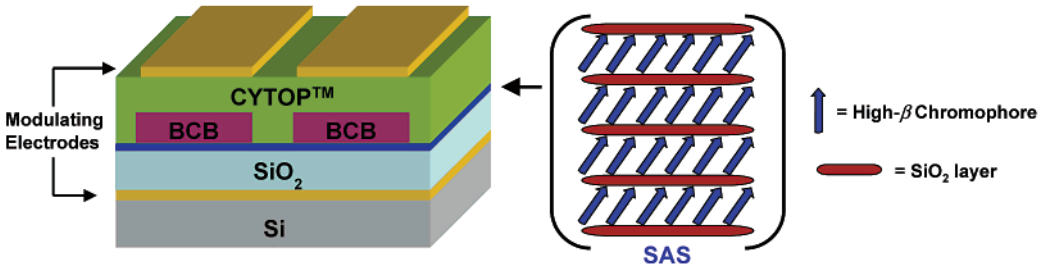

[a] The commercially available, electronic-grade glassy polymers Cytop (a fluorinated polyether) and BCB (=polybisbenzocyclobutane; also known as Cyclotene) are used as low-index cladding and SAS index-matched low-loss waveguiding materials, respectively.

Scheme 2. Schematic Representation of the Two-Step Layer-by-Layer Self-assembly of 3-Based Self-assembled Superlattices[a]

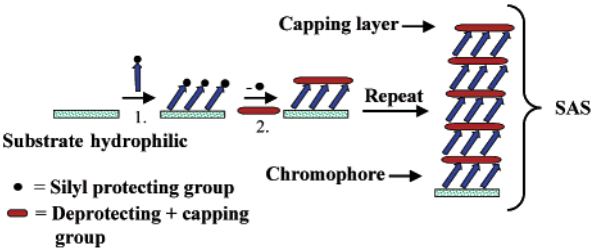

[a] The procedure can be performed by use of a single-reaction vessel and standard cannula techniques or by immersion of the substrates in reagent and washing of solutions within a nitrogen-filled glove bag.

steps) are required for this particular procedure. Therefore, to be practical, the procedure must be automated and should equal or surpass other well-established layer-by-layer growth techniques (e.g., LB methods) in terms of film microstructural regularity, growth efficiency, and flexibility. In the three-step "first-generation" procedure,[12c,d,13k] a coupling layer such as 3-bromopropyltrichlorosilane, or [(4-chloromethyl)phenyl]trichlorosilane, is first self-assembled onto substrates such as sodium lime glass or a single-crystal silicon wafer. Second, the chromophore is covalently linked to the coupling layer through an inefficient quaternization reaction. Third, a planarizing capping layer is deposited. Since the chemisorptive quaternization reaction is very slow, alternative spin-coating followed by vacuum oven treatment at 110 °C are necessary to obtain full chromophore coverage.[12c,d] This step clearly represents a serious impediment to automating the growth process.

In this contribution, we describe a greatly improved all-"wet-chemical" approach to the expeditious, straightforward self-assembly[16] of these large-response optically/electronically functional siloxane-based SAS films using reactive $-SiCl_2I$ derivatives of a protected azobenzene chromophore and a chlorosiloxane deprotecting/capping reagent (Scheme 2). We show that the film assembly time is now comparable to LB and related layer-by-layer deposition techniques[13] and more than an order of magnitude more rapid than our previously employed methods,[9−12] thus offering methodology for depositing thicker self-assembled EO films. Specifically, the deposition technique reported here employs the iterative combination of *only two steps*: (i) Self-limiting polar chemisorption of a protected model high-β chromophore monolayer ($t \sim 15$ min) and (ii) in situ trialkylsilyl group removal, plus self-limiting capping of each chromophore layer using octachlorotrisiloxane ($t \sim 25$ min; Scheme 2). This latter step deposits a robust polysiloxane layer which stabilizes the polar microstructure via interchromophore cross-linking and regenerates a reactive hydrophilic surface.[9−12,18] The use of a model high-β azobenzene chromophore not only affords a large EO response but also enables second-harmonic generation (SHG) spectroscopic measurements as an additional analytical tool to verify the polar regularity of SAS evolution afforded by this efficient deposition method. It will be seen that this two-step, layer-by-layer synthetic approach affords thermally robust[12d] superlattices exhibiting large NLO/EO responses ($\chi^{(2)} \sim 180$ pm/V, $r_{33} \sim 65$ pm/V at 1064 nm) and can be efficiently carried out in any synthetic organic chemistry laboratory in a single-reaction vessel using standard cannula techniques or by consecutive vertical dipping of the substrates in recyclable reaction solutions using a simple nitrogen-filled glove bag. Comparable or more sophisticated tools are needed for many other layer-by-layer assembly methods.

Experimental Section

Materials and Methods. The synthesis, purification, and characterization of 4-[4-*N*,*N*-bis(*tert*-butyldimethylsiloxyethyl)-aminophenylazo]pyridine has been reported previously.[12c] Unless stated otherwise, chemicals were purchased from Aldrich Chemical Co. and used as received. Trichloro(4-chloromethyl)-phenylsilane was distilled under vacuum before use. NaI was flame-dried under high vacuum and then heated at 140 °C in vacuo for an additional 24 h prior to use. Acetonitrile was distilled from P_2O_5. Pentane (Fisher Scientific) and heptane (Fisher Scientific) were dried by passing them through a purification column. The solvents CH_2Cl_2 and THF were distilled under N_2 from CaH_2 and Na/K alloy, respectively. Octachlorotrisiloxane and single-crystal silicon (111) substrates were purchased from Gelest and Semiconductor Processing Company, Inc., respectively. Sodium lime glass and silicon wafer substrates were cleaned by immersion in "piranha" solution (H_2SO_4/30% H_2O_2 7:3 (v/v)) at 80 °C for 1 h. (*Caution: piranha solution is a dangerous oxidizing agent and should be handled with care using appropriate shielding.*) After being cooled to room temperature, the substrates were rinsed with deionized water and then subjected to an RCA-type cleaning protocol ($NH_3 \cdot H_2O/H_2O/30\%$ H_2O_2 1:5:1 (v/v) at room temperature, 40 min). They were then washed with deionized water and dried in an oven (125 °C) overnight. The growth of chromophoric superlattices was carried under an inert atmo-

(18) Malinsky, J. E.; Jabbour, G. E.; Shaheen, S. E.; Anderson, J. D.; Richter, A. G.; Marks, T. J.; Armstrong, N. R.; Kippelen, B.; Dutta, P.; Peyghambarian, N. *Adv. Mater.* **1999**, *11*, 227−231.

sphere using either standard Schlenk/cannula techniques or in a N_2-filled glove bag, which was continuously purged (see details below).

NMR spectra were recorded on a Varian-300 or Mercury-400 spectrometer. UV−vis spectra were recorded with a Cary 1E spectrophotometer. Elemental analyses were performed by Midwest Microlabs. Advancing contact angles were measured on a standard goniometric bench fitted with a Teflon micrometer syringe (Gilmont Instruments, Inc.). Polarized second-harmonic generation measurements were carried in the transmission mode with a Q-switched Nd:YAG laser operating at 1064 nm, with a pulse width of 3 ns at a frequency of 10 Hz. Details of the instrumentation and calibration procedures can be found elsewhere.[11] X-ray reflectivity measurements were carried out on Beamline X23B of National Synchrotron Light Source at Brookhaven National Laboratory. Data requisition and analysis procedures are described elsewhere.[11] Atomic force microscopic images were recorded with a Nanoscope II instrument (Digital Instruments, Inc.).

1. Synthesis of 4-(4-{Bis-[2-(*tert*-butyldimethylsilanyloxy)-ethyl]-amino}-phenylazo)-1-[4-(dichloro-iodo-silanyl)-benzyl]pyridinium iodide (3). *(a) Synthesis of Dichloroiodo-(4-iodomethyl)phenylsilane **2**.* An air-free 100-mL flask was charged with dry NaI (5.6 g, 40 mmol), dry acetonitrile (30 mL), and trichloro(4-chloromethyl)phenylsilane (1.1 mL, 10 mmol). A white suspension formed instantly, and the mixture was stirred under an inert atmosphere at room temperature for 19 h with exclusion of light. The solvent was then removed at ≈60 °C under vacuum. Subsequently, the product was extracted with dry pentane (3 × 50 mL) and transferred via cannula into another air-free flask. An extremely air-sensitive white solid was obtained after removal of the volatiles (yield, 90%). ^{1}H NMR (300 MHz, CD_2Cl_2): δ 7.71 (d, 2H, J = 6.6 Hz), 7.45 (d, 2H, J = 6.6 Hz), 4.46 (s, 2H).

*(b) Synthesis of 4-(4-{Bis-[2-(tert-butyldimethylsilanyloxy)-ethyl]-amino}-phenylazo)-1-[4-(dichloro-iodo-silanyl)-benzyl]-pyridinium iodide **(3)**.* An air-free flask (100 mL) was charged with reagent **1**[12c] (5.14 g, 100 mmol), dry CH_2Cl_2 (10 mL), and dichloroiodo[(4-iodomethyl)phenyl]silane (**2**; 4.43 g, 100 mmol). The red mixture was heated under an inert atmosphere at 60 °C for 4 h with exclusion of light. The solvent was then removed under high vacuum and the residue dried under high vacuum overnight. Yield: 9.57 g (100%) of dark purple solid. ^{1}H NMR (400 MHz, CD_2Cl_2): δ 9.12 (d, 2H, J = 6.0 Hz), 8.06 (s, 2H), 7.96 (s, 2H), 7.85 (d, 2H, J = 7.2 Hz), 7.77 (d, 2H, J = 7.6 Hz), 6.94 (d, 2H, J = 8.8 Hz), 6.16 (s, 2H), 3.87 (t, 4H, J = 3.6 Hz), 3.77 (t, 4H, J = 3.6 Hz), 0.84 (s, 18 H), 0.00 (s, 12 H). Anal. Calcd for $C_{34}H_{52}Cl_2I_2N_4O_2Si_3$: C, 42.64; H, 5.47; N, 5.85. Found: C, 42.38; H, 5.39; N, 5.62.

2. Growth of Self-assembled Superlattices. The following procedure can be carried out in a single-reaction vessel using standard cannula techniques to transfer the solutions. An equally efficient dipping procedure can be used as well. In the latter case, all reagents, reaction solvents, and washing solvents are contained in a glove bag, which is continuously purged with prepurified N_2. In both procedures, the substrates are fixed in a Teflon sample holder and fully immersed in the appropriate reaction or rinsing solutions. Substrates were dried using a flow of N_2.

(i) Self-assembly of Chromophore **3**. Under N_2, freshly cleaned ITO, sodium lime glass, and/or silicon substrates were loaded into the Teflon sample holder and immersed in a THF solution of **3** (10 mM) at 55 °C for 15 min. The resulting purple substrates were then rinsed with THF and sonicated in methanol for 2 min.

(ii) Capping with Octachlorotrisiloxane. Under N_2, the substrates were immersed in a dry pentane solution of octachlorotrisiloxane (34 mM) at room temperature for 25 min, rinsed twice with dry pentane and then acetone, and sonicated in methanol for 2 min. Chromophore **3** and octachlorotrisiloxane solutions can be used for at least 10 repetitions without noticeable degradation or compromise of SAS properties.

Results and Discussion

Synthesis of Reactive −SiCl$_2$I-Functionalized SAS Chromophore Building Blocks (3). Reaction of chromophore precursor 4-[*N*,*N*-bis(*tert*-butyldimethylsiloxyethyl)amino]-phenylazopyridine **1** with dichloroiodo(4-iodomethyl)phenylsilane **2** in dry CH_2Cl_2 results in quantitative formation of the new purple, siloxy-protected chromophore reagent 4-(4-{bis-[2-(*tert*-butyl dimethylsilanyloxy)-ethyl]-amino}-phenylazo)-1-[4-(dichloro-iodo-silanyl)-benzyl]pyridinium iodide **3** (eq 1), which

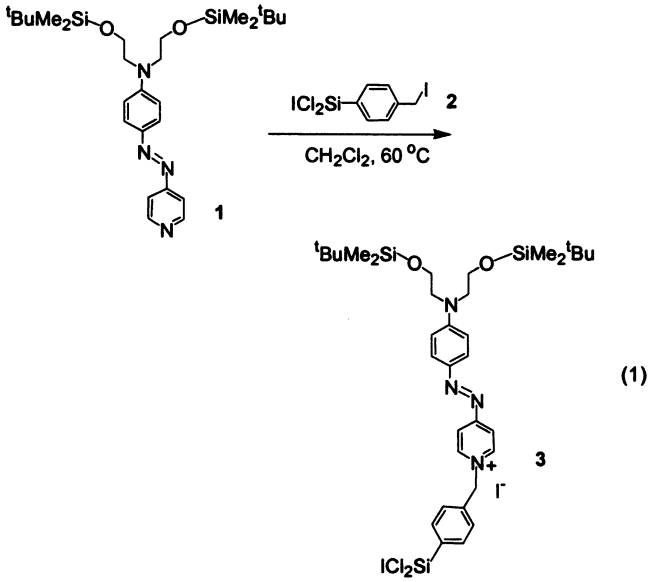

(1)

was fully characterized by conventional analytical techniques. Alkylpyridinium-based chromophores akin to **3** have similar spectroscopic properties (e.g., the optical spectra of such quaternized donor−acceptor salts exhibit characteristic ≈90-nm red shifts of the charge-transfer excitation band vs the netural chromophore precursor).[9a,b]

Monolayer, Bilayer Formation Monitored by Transmission Optical and Second-Harmonic Generation Spectroscopy. Chromophore deposition kinetics from THF solution onto clean float-glass substrates were first monitored by UV−vis and SHG spectroscopy to optimize reaction conditions. The chromophore HOMO−LUMO CT optical transition at λ = 575 nm and the 532-nm SHG light output intensity ($I^{2\omega}$) reach a maximum after ≈15 min at 55 °C (10 mM in THF). Figure 1 shows the deposition kinetics at 50 °C (8.0 mM in THF). Longer reaction times result in a slight decrease in $I^{2\omega}$, while the optical absorbance at 575 nm remains constant. The reason for the decline in $I^{2\omega}$ at longer reaction times is presently unknown and may be the result of evolution in the chromophore tilt angle or slow structural degradation (e.g., trialkylsilyl group removal) of the monolayer by evolved HX (X = Cl, I) formed via reaction of the chromophore with the hydrophilic surface and/or with adventitious H_2O. Variation in chromophore tilt angle as a function of coverage during monolayer formation has been observed in other self-assembling systems.[12d] No hypsochromic shifts are observed in the present optical absorption spectra, arguing that centrosymmetric H-type chromophore aggregation is not important. The formation of such aggregrates adversely affects the EO response of certain

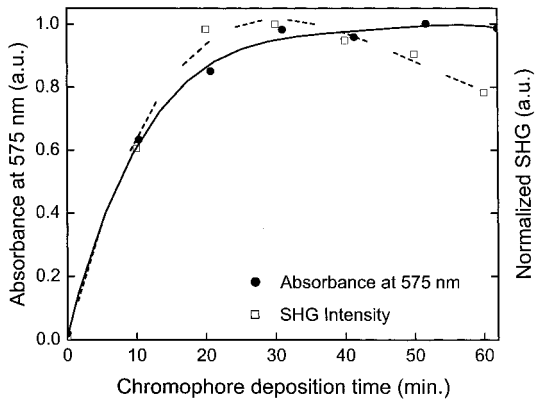

Figure 1. Optical spectroscopic data and second-harmonic generation (SHG) response measurements as a function of reaction/deposition time for the formation of a **3**-based chromophore monolayer from THF solution (8.0 mM **3**, 50 °C) on a float glass substrate.

LB film structures,[19] and the degree of aggregration for a specific chromophore is highly dependent on the particular film growth technique.[19a] Protonation of the present films seems less likely since no shift in λ_{max} is observed. Furthermore, aqueous contact angle (CA) measurements on the chromophore-functionalized substrates (step 1, Scheme 2) reveal hydrophobic surfaces ($\theta_a \sim 76°$) in accordance with the formation of densely packed organic films, exposing only the trialkylsilyl protecting groups at the outer surface.

With regard to the concurrent deprotection and capping process (step 2, Scheme 2), previous studies established that reaction of similar films with THF solutions of $^nBu_4N^+F^-$ results in rapid protecting group removal, yielding reactive, hydrophilic surfaces.[9−11] Although speculative, we hypothesize that the present reaction of octachlorotrisiloxane in dry pentane with the hydrophobic surface (and traces of adsorbed H_2O) effects in situ chromophore deprotection and formation of a hydrophilic polysiloxane surface (step 2, Scheme 2). Octachlorotrisiloxane is a strong Lewis acid and reacts instantly with traces of H_2O, forming HCl. The latter would deprotect the trialkylsilyl-terminated chromophore layer in situ and may also catalyze polysiloxane condensation.[20,21] In support of this suggestion, we find that reaction of trialkylsilyl-protected chromophore films with ethanolic HCl solutions indeed results in rapid deprotection.[22] It will be seen that the result of this two-step synthetic methodology is a substantial reduction in the time required to achieve smooth, structurally regular polysiloxane-capped chromophore bilayers (vide infra).

SAS Multilayer Formation and Characterization. The present iterative two-step chemisorptive SA process (Scheme 2) and the resulting multilayer structural regularity have been characterized by a full complement of physicochemical techniques: optical transmission spectroscopy (to characterize assembly chemistry and microstructural regularity), advancing aqueous contact angle measurements (to characterize surface energy/wettability), synchrotron X-ray reflectivity (XRR; to characterize film thickness, density, and interfacial roughness), atomic force microscopy (to characterize surface morphology and roughness), and angle-dependent polarized SHG spectroscopy (to characterize NLO/EO response, microstructure, polar regularity). The thermally and photochemically robust SAS films derived from the new assembly procedure of Scheme 2 adhere strongly to hydrophilic substrates (e.g., glass, silicon), cannot be detached from the surface by the standard "Scotch tape" decohesion test, and are unaffected by common organic solvents. The films are, however, etched by HF solutions. Chromophore and octochlorotrisiloxane solutions can be reused ≈10 times without any noticeable detrimental effects on film quality. Aqueous CA measurements on each bilayer show a continual regeneration of a constant density of reactive hydroxyl surface sites ($\theta_a \sim 39°$) after step 2 of Scheme 2, which is a necessary requirement for the covalent assembly of the chromophore monolayers and sequential buildup of structurally uniform siloxane-based multilayers.

SAS X-ray Reflectivity. Specular X-ray reflectivity was used to probe the microstructural evolution and details of the SAS films. Data for a series of 1−5 bilayers were obtained by fitting the multilayer reflectivity data to a Gaussian-step model.[11,23] In general, X-ray specular reflectivity is a function of the electron density profile $\rho(z)$ perpendicular to the sample surface. For the present systems, a model consisting of a silicon substrate and layers of different electron densities, ρ_i, with Gaussian broadened interfaces, σ_i, was used (eq 2).[11,23c] Here, the

$$\frac{R(q_z)}{R_F(q_z)} = \left| \sum_{i=0}^{N} \frac{(\rho_i - \rho_{i+1})}{\rho_0} e^{-iq_z D_i} e^{-q_z^2 \sigma_{i+1}^2/2} \right|^2 \qquad (2)$$

wave vector transfer $|\mathbf{q}| = q_z = (4\pi/\lambda) \sin\theta$ is along the surface normal, $R_F(q_z)$ is the theoretical Fresnel reflectivity for an ideally flat substrate surface, N is the number of layers, ρ_0 is the electron density of the substrate ($=\rho_{Si}$), $D_i = \sum_{j=1}^{i} T_j$ is the distance from the substrate surface to the ith interface, and T_i is the thickness of the ith layer. The reflectivity data were fit to such a model, the fitting parameters being the thickness and the electron density of each layer, and the root-mean-square width of each interface. Equation 2 is valid for q_z larger than approximately twice the critical wave vector for total external reflection ($q_c = 0.0316$ Å^{-1} for Si), where refraction effects are negligible. Thus, the fits were performed using only data for which $q_z > 2q_c$. Figure 2 shows normalized reflectivity data (R/R_F) from a typical scan on a three-bilayer film. The solid line shows the best fit using eq 2. The

(19) (a) Facchetti, A.; van der Boom, M. E.; Abbotto, A.; Beverina, L.; Marks, T. J.; Pagani, G. A. *Langmuir* **2001**, *17*, 5939−5942. (b) Carpenter, M. A.; Willard, C. S.; Penner, T. L.; Williams, D. J.; Mukamel, S. *J. Phys. Chem.* **1992**, *96*, 2801−2804.

(20) Cabibil, H.; Celio, H.; Lozano, J.; White, J. M.; Winter, R.*Langmuir* **2001**, *17*, 2160−2166.

(21) (a) Nijmeijer, A.; Kruidhof, H.; Bredesen, R.; Verweij, H. *J. Am. Ceram. Soc.* **2001**, 84, 136−140. (b) Krongelb, S. *Electrochem. Technol.* **1968**, *6*, 251−256.

(22) van der Boom, M. E.; Marks, T. J., unpublished observations. The RO−$SiMe_2{}^t$Bu bonds are expected to be unstable toward Brønsted acids; see: *Protecting Groups in Organic Synthesis*, 2nd ed.; Greene, T. W., Wuts, P. G. M., Eds.; John Wiley & Sons: New York, 1991.

(23) (a) Tidswell, I. M.; Ocko, B. M.; Pershan, P. S. *Phys. Rev. B* **1990**, *41*, 1111−1127. (b) Pomerantz, M.; Segmuler, A.; Netzer, L, Sagiv, J. *Thin Solid Films* **1985**, *132*, 153−162. (c) Tidswell, I. M.; Rabedeau, T. A.; Pershan, P. S.; Kosowsky, S. D.; Folkers, G. P.; Whitesides, G. M. *J. Chem. Phys.* **1991**, *95*, 2854.

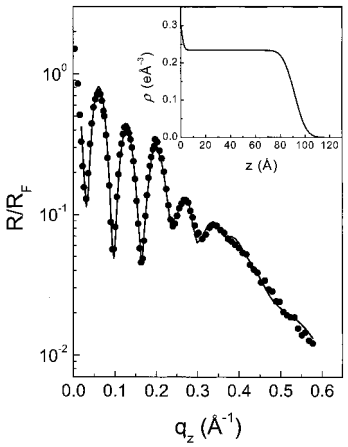

Figure 2. Specular X-ray reflectivity (XRR) data for a **3**-based three-bilayer sample prepared via the procedure of Scheme 2. The solid line shown is the best fit to the data. Inset: the corresponding electron density profile obtained from this fit.

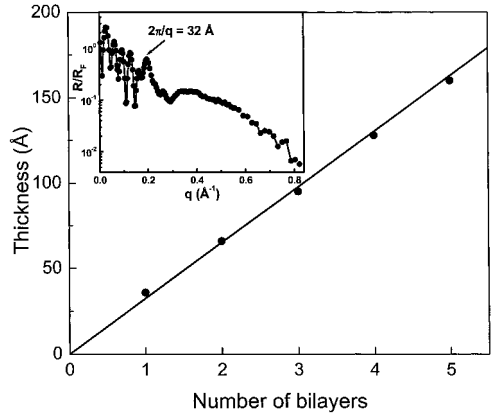

Figure 3. Specular X-ray reflectivity (XRR)-derived film thickness (Å) data as a function of the number of **3**-based bilayers prepared via the procedure of Scheme 2. The solid line is the fit by linear regression, indicating an average interlayer spacing of 32.6 Å. Inset: XRR data for a 5-bilayer sample. The solid line shown is the best fit to the data. The "Bragg" feature independently yields an interlayer spacing of ≈32 Å.

corresponding electron density profile obtained from this fit is presented in the inset of Figure 2. Similar reflectivity patterns and electron density profiles were obtained for all samples (for example, see the reflectivity data for the five-bilayer sample in the inset of Figure 3). The SAS X-ray reflectivity data exhibit pronounced minima, "Kiessig fringes" (Figures 2 and 3),[9−12,24] corresponding to destructive interference of reflections from the multilayer substructure of the film and indicating a narrow distribution of layer thicknesses. Variation in layer thicknesses would smear out the first-order fringe,[25] which is not observed here. It can be seen that the film thickness (D_{film}) increases linearly as a function of the number of bilayers (Figure 3), underscoring the high structural regularity and efficiency of this synthetic approach. An average interlayer spacing of 32.6 Å can be deduced from the slope of the line obtained by linear regression. The "Bragg" peak in the reflectivity due to scattering by identical layers also yields an interlayer spacing of about 32 Å (Figure 3; inset), meaning that these films are extremely well-ordered in the surface normal direction, although there are small density variations between the interlayers.

"Bragg" peaks have been observed previously in highly ordered Langmuir−Blodgett films and covalently bonded self-assembled multilayers.[9−12,24] It is known that relatively small structural variations in layered structures can significantly broaden or eliminate the Bragg features. The present XRR measurements further reveal that the films have well-defined interfaces, consistent with good structural ordering as also indicated by the UV−vis and SHG data (Figures 4 and 5; vide infra). The XRR-derived surface roughness ($\sigma_{film-air}$ widths) varies from 6.5 to 14 Å and the behavior of the relative surface roughness, defined as $\sigma_{film-air}/D_{film}$, decreases to ≈8% upon multilayer formation. On the basis of the electron density profiles obtained, we have calculated the number of electrons per unit of substrate area for one bilayer, $N_{film,exp}$, according to $N_{film,exp} = \int \rho(z)\, dz$, where the integration is taken over the whole film. The molecular footprint is calculated as $N_{mol}/N_{film,exp}$, where N_{mol} is the calculated number of electrons in one molecular unit, using the chemical formula of the chromophore and the capping layer. In the case of two or more bilayers, $N_{film,exp}$ is calculated for the entire film and N_{mol} is the quantity of electrons in one molecular unit (=chromophore + capping layer) multiplied by the number of bilayers. Importantly, these estimations show that the molecular "footprint" of ≈40 Å^2/chromophore remains constant upon multilayer formation.

Optical UV−Vis Spectroscopy. Homogeneous substrate coverage within the 2.5 × 2.5 cm^2 substrate surface area and deepening of the purple color of the SA films assembled on transparent surfaces upon repeating the two deposition steps can be clearly observed by the eye. UV−vis measurements unambiguously evidence a linear dependence of the HOMO−LUMO CT chromophore optical absorbance at $\lambda = 575$ nm on the number of bilayers, demonstrating that essentially equal quantities of uniformly aligned chromophore units are incorporated in each sublayer up to 40 bilayers (Figure 4). No other bands or shifts in the optical absorbance maxima are observed, arguing against significant chromophore aggregation or decomposition.

Second-Harmonic Generation Spectroscopy. Polarized transmission SHG measurements on the present SAS structures at $\lambda_0 = 1064$ nm were carried out on samples placed on a computer-controlled rotation stage, enabling the incidence angle of the input radiation to the sample surface normal to be varied from 0° to 70°. Angle-dependent SHG interference patterns for glass substrates coated on both sides with SAS films demonstrate that the two-step deposition process affords identical film quality and uniformity on both sides of the substrate (Figure 5; inset). A quadratic dependence of the 532-nm light output intensity ($I_{obs}^{2\omega}$) on the number of bilayers is observed for thin samples (20 or less bilayers; Figure 5). However, for thicker samples, SHG response intensities exhibit a saturation effect due, at least in part, to self-absorption of the samples at 532

(24) (a) Richter, A. G.; Durbin, M. K.; Yu, C.-J.; Dutta, P. *Langmuir* **1998**, *14*, 5980−5983. (b) Malik, A.; Durbin, M. K.; Richter, A. G.; Huang, K. G.; Dutta, P. *Phys. Rev. B* **1995**, *52*, 11654−11657.

(25) Naifan, N.; Parrat, L. G. *J. Appl. Phys.* **1960**, *31*, 1331−1337.

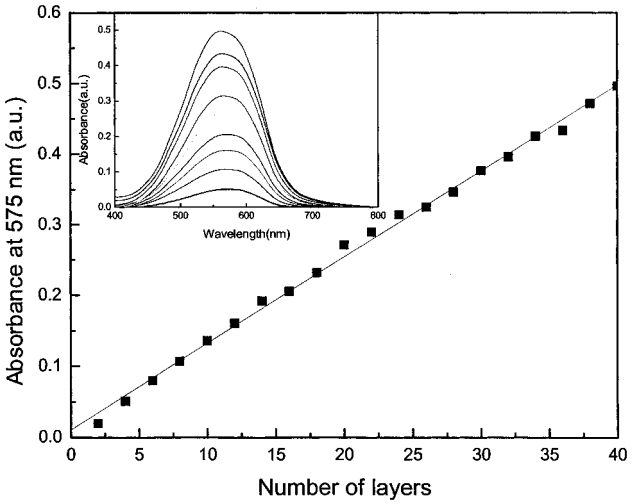

Figure 4. Optical absorption spectra of SAS films at 575 nm as a function of the number of **3**-based bilayers. The solid line is the fit by linear regression. Inset: UV−vis absorption spectra of 4, 8, 12, ..., 40 bilayer samples.

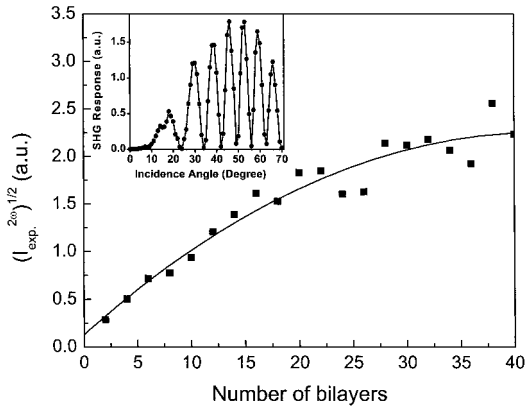

Figure 5. Square-root of SAS film 532-nm second-harmonic generation (SHG) response ($I_{exp.}^{2\omega}$, arbitrary units) as a function of the number of **3**-based bilayers. The solid line is drawn as a guide to the eye. Inset: SHG response as a function of fundamental beam incident angle from a float glass slide having a SAS bilayer on either side.

nm (Figure 4 inset). This self-absorption was corrected using eq 3,[26]

$$\chi^{(2)} = \chi^{(2)}_{obs} \exp(\alpha l/4)(\alpha l/4)/\sinh(\alpha l/4) \qquad (3)$$

where $\chi^{(2)}_{obs}$ is the observed, uncorrected $\chi^{(2)}$ value, α is the absorption coefficient, and l is the film thickness. A quadratic dependence of the absorption-corrected I^2 on the number of bilayers (Figure 6) indicates the preservation of a polar microstructure as the layer-by-layer assembly progresses. For a regular, polar multilayer the light output intensity ($I^{2\omega}$) should scale quadratically with the number of layers because the incident light wavelength (1064 nm) is large compared to the film thickness ($l \sim 32.6 \times n$ Å; n = number of bilayers).[27] The multilayer SAS films exhibit large second-order macroscopic EO responses, $\chi^{(2)} \sim 180$ pm/V, which doubtless reflects non-negligible resonant enhancement

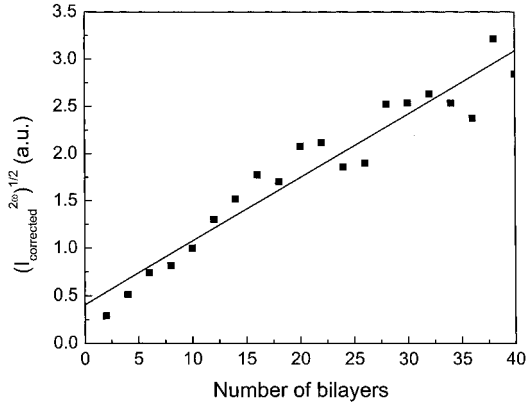

Figure 6. Absorption-corrected square root of SAS 532-nm SHG response ($I_{corrected}^{2\omega}$; eq 3) as a function of the number of **3**-based bilayers. The line through the data points has been fit by linear regression.

as established previously.[12d,28] Since the present films are too thin for measurement of the electro-optic coefficient by conventional reflectometry,[29] the EO coefficient r_{33} was estimated from the SHG response to be ≈65 pm/V at 1064 nm by calibration vs quartz and known EO films using the established[6c,30] relationship $r_{33} = -2\chi^{(2)}_{zzz}/(n_z)^4$. The chromophore number density is estimated using $N_s = (l \times \chi^{(2)}_{zzz})/(\beta_{zzz} \times \cos^3 \Psi)$.[12c] This relationship of course assumes a narrow distribution of molecular tilt angles.[23] Note, however, that the SHG-derived tilt angle, $\Psi \sim 40°$, is close to the so-called magic angle.[31] An average chromophore surface density, $N_s \sim 2.5 \times 10^{12}$ molecules/cm^2, is estimated for each bilayer using the ZINDO-derived chromophore molecular hyperpolarizability β_{zzz} at 1064 nm,[12c] the experimental $\chi^{(2)}_{zzz}$, and the average interlayer spacing ($l = 32.6 \times n$ Å; n = number of bilayers). The derived N_s corresponds to an average "footprint" of ≈40 Å^2/chromophore, which compares favorably with the XRR-derived "footprint" (vide supra) and those reported for SA and LB films containing structurally similar chromophore building blocks.[9−12,32]

Atomic Force Microscopy. Contact mode AFM measurements on 10- and 40-bilayer SAS samples reveal a slightly grainy texture and an rms surface roughness of ≈2.7 and ≈9.9 nm, respectively, for 1 × 1 μm^2 scan areas (Figure 7). The relative film roughness (rms roughness/film thickness) remains constant at ≈8%. Grain formation is a common,[10,11] but still poorly, understood phenomenon in films fabricated using layer-by-layer assembly processes. Scanning force microscopy studies of related organic−inorganic hybrid films prepared with group 13 oxide interlayers and group IV metal-coordination based SASs reveal somewhat similar grain-type topographies.[10,11,13]

(26) Amano, M.; Kaino, T. *J. Appl. Phys.* **1990**, *68*, 6024−6028.
(27) Bloembergen, N.; Pershan, P. S. *Phys. Rev.* **1962**, *128*, 606−622.
(28) Lundquist, P. M.; Yitzchaik, S.; Zhang, T.; Kanis, D. R.; Ratner, M. A.; Marks, T. J.; Wong, G. K. *Appl. Phys. Lett.* **1994**, *64*, 2194−2196.
(29) (a) Teng, C. C.; Man, H. T. *Appl. Phys. Lett.* **1990**, *56*, 1734−1737. (b) Schildkraut, J. S. *Appl. Opt.* **1990**, *29*, 2839−2847.
(30) Shuto, Y.; Amano, M. *J. Appl. Phys.* **1995**, *77*, 4632−4638.
(31) Simpson, G. J.; Rowlen, K. L. *J. Am. Chem. Soc.* **1999**, *121*, 2635−2636.
(32) Ashwell, G. J.; Hargreaves, R. C.; Baldwin, C. E.; Bahra, G. S.; Brown, C. R. *Nature* **1992**, *57*, 393−394.

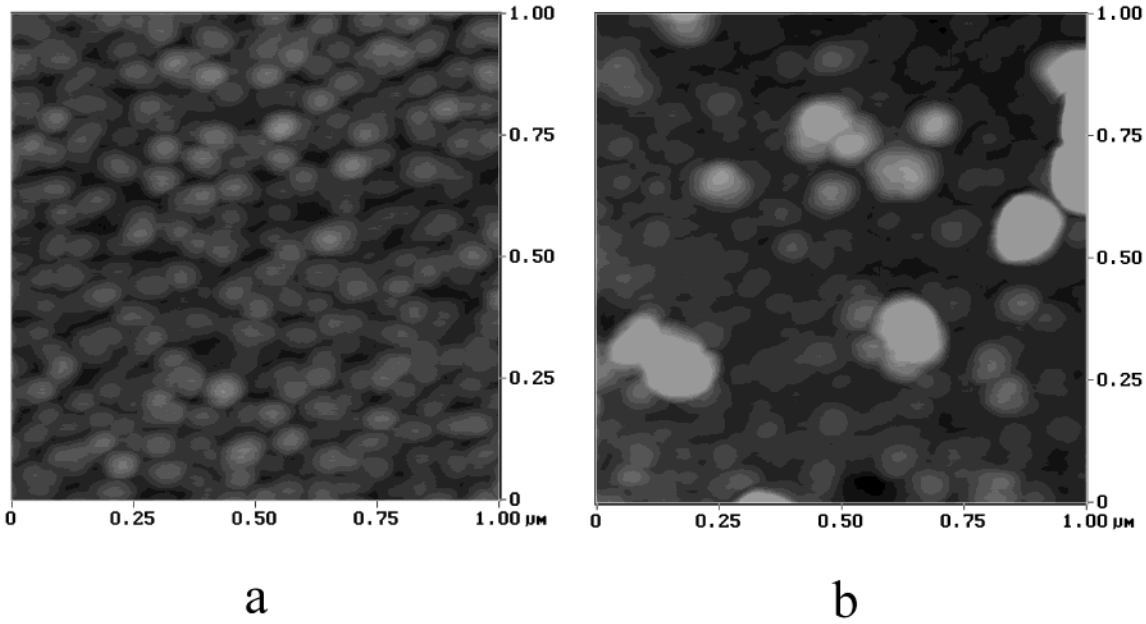

Figure 7. AFM images at a 1 × 1 μm scan area of an SAS structure composed of (a) 10 and (b) 40 bilayers.

Conclusions

The present two-step self-assembly technique using a highly reactive $-SiCl_2I$-functionalized chromophore demonstrates an expeditious and efficient approach to the formation of nanoscopically acentric films of known materials having sizable, intrinsic EO responses. This streamlined thin film growth process results in structurally regular multilayers with each ≈3.26-nm-thick bilayer conveniently grown from recyclable solutions using a single-reactor process or by an even more straightforward vertical dipping procedure. The present streamlining to 40 min/bilayer represents a major improvement over our earlier procedure (≈6 h/layer) but should not be construed as the ultimate in efficiency, and it is likely that further optimization in methodology will be possible. Such a procedure is in principle compatible with parallel growth on multiple substrates or on large substrates which are subsequently cut. The time scale is unlikely to be terribly different from that for the hydrothermal growth, cutting, and polishing of modulator-quality $LiNbO_3$ crystal slices.[14]

We have demonstrated here the formation of structurally regular, polar films consisting of up to 40 alternating chromophore and capping layers. The present film quality, assembly time, chromophore density and microstructural polarity, and experimental simplicity are comparable to well-known layer-by-layer techniques, which are based on relatively weak interactions between chromophore layers (i.e., hydrogen bonding, van der Waals interactions, or electrostatic forces). The large numbers of strong, covalent Si−O bonds renders the present films chemically and thermally durable. Indeed, for such a quality of film microstructure, robustness, and morphology, this growth rate rivals or exceeds that of other typical solution-phase layer-by-layer growth processes.[4,13,32] No postdeposition steps such as cross-linking of specially designed building blocks to enhance thermal stability are required. Moreover, film deformation due to evaporation of included solvents is not observed. The potentially automatable process demonstrated here with a model azobenzene chromophore should be applicable to a wide range of electro-optic and other chromophores and provides an unprecedented level of accessibility to intrinsically polar molecular EO materials for future photonic devices. We will describe these results in future contributions.

Acknowledgment. This research was supported by the NSF under Grant DMR-0076077 (NSF MRSEC program through the Northwestern Materials Research Center) and by ARO/DARPA under Contract DAAD 19-00-1-0368. X-ray reflectivity measurements were performed at Beam Line X23B of the National Synchrotron Light Source, which is supported by the U.S. Department of Energy. We also thank Dr. Bo Liu and Professor Mark G. Kuzyk for helpful discussions on absorption corrections for SHG measurements.

CM020438T